THE IMPACT OF TOGA TAO WIND OBSERVATIONS ON TROPICAL PACIFIC OCEAN SIMULATIONS

C. Menkes[1,3] and A.J. Busalacchi[2]

(1) Laboratory for Hydrospheric Processes, USRA/GSFC, Greenbelt, MD 20771, U.S.A.
(2) Laboratory for Hydrospheric Processes, NASA/GSFC, Greenbelt, MD 20771, U.S.A.
(3) Groupe SURTROPAC, ORSTOM, Nouméa, NEW CALEDONIA

INTRODUCTION

During the TOGA decade, it became quite apparent that uncertainties in the surface wind field observations across the Pacific Ocean were one of the most serious impediments to advances in ENSO prediction studies. In response to the need for better wind observations, and together with measurements of the subsurface thermal structure, the TOGA-TAO array has become the most important element of the TOGA Observing System. As the TOGA Program concludes, plans are being made to stabilize the present array, implement a program to evaluate the optimum configuration needed to support useful ENSO forecasts, and develop criteria for future expansion. Yet, very little has been done so far to assess the impact TAO wind observations have had on operational analysis from numerical weather prediction centers. To estimate what that impact might, a series of linear ocean model hindcasts are performed in the equatorial Pacific with different wind data sets in which TAO wind observations are combined.

WIND FORCINGS

The baseline forcings for this study include the FSU pseudo-stress product (converted to stress using a constant drag coefficient of 1.2×10^{-3}) and an AMIP-type wind product from the National Meteorological Center (NMC, courtesy of Ming Ji) for the 1982-1993 period. The AMIP wind from 9 ensemble averages is similar to the one used in Ji and Smith (1995) except that here, the interannual anomalies are combined to Hellerman and Rosenstein's (1993) climatology decreased by a factor 0.8. This wind is representative of the quality of the operational analysis prior to data assimilation and is referred to as AMIP9 in the following.

Subsequently, the TAO stresses are merged with the prior data via optimal interpolation as follows : TAO stresses are computed from TAO winds, air temperature, sea surface temperature and relative humidity using the Liu et al. (1979) formulas at each TAO mooring. The daily stresses are then monthly averaged and the stress residuals (TAO-FSU) and (TAO-AMIP9) are computed at TAO moorings and interpolated to the baseline forcing fields with optimal interpolation. These residuals have increasingly detailed spatial structures as the TAO array is gradually implemented (Figure 1) and comes to its near full development in 1993 (Figure 2). Lastly, the residuals are added back to the baseline forcings yielding two presumably improved stress data sets AMIP9+TAO and FSU+TAO.

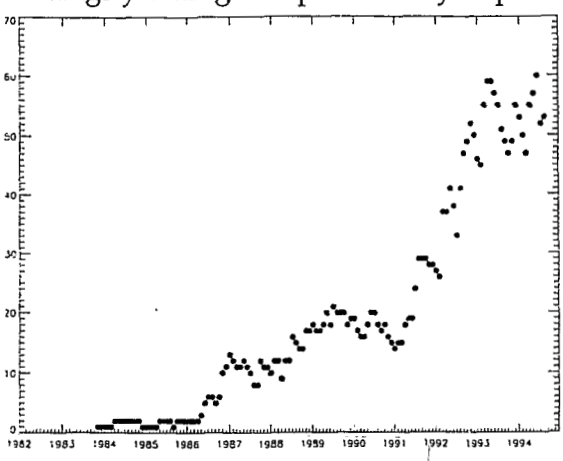

Figure 1 - Number of TAO wind observations available per month during TOGA

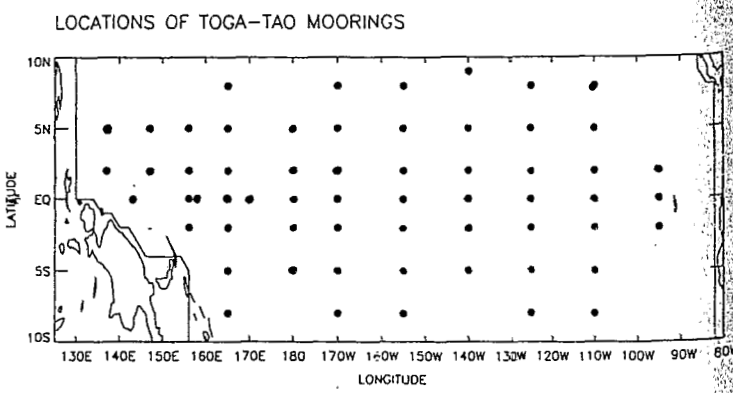

Figure 2 - The TAO array fully developed

As illustrated in the wind stress time series at EQ/165°E (Figure 3), the addition of TAO stress remedies some of the deficiencies in the AMIP9 stress which is too easterly and lacks the strong westerly wind bursts observed by TAO (Figure 3a-b). Similarly, the addition of TAO winds to FSU brings back the westerly wind activity missed by FSU in late 91 (Figure 3c-d).

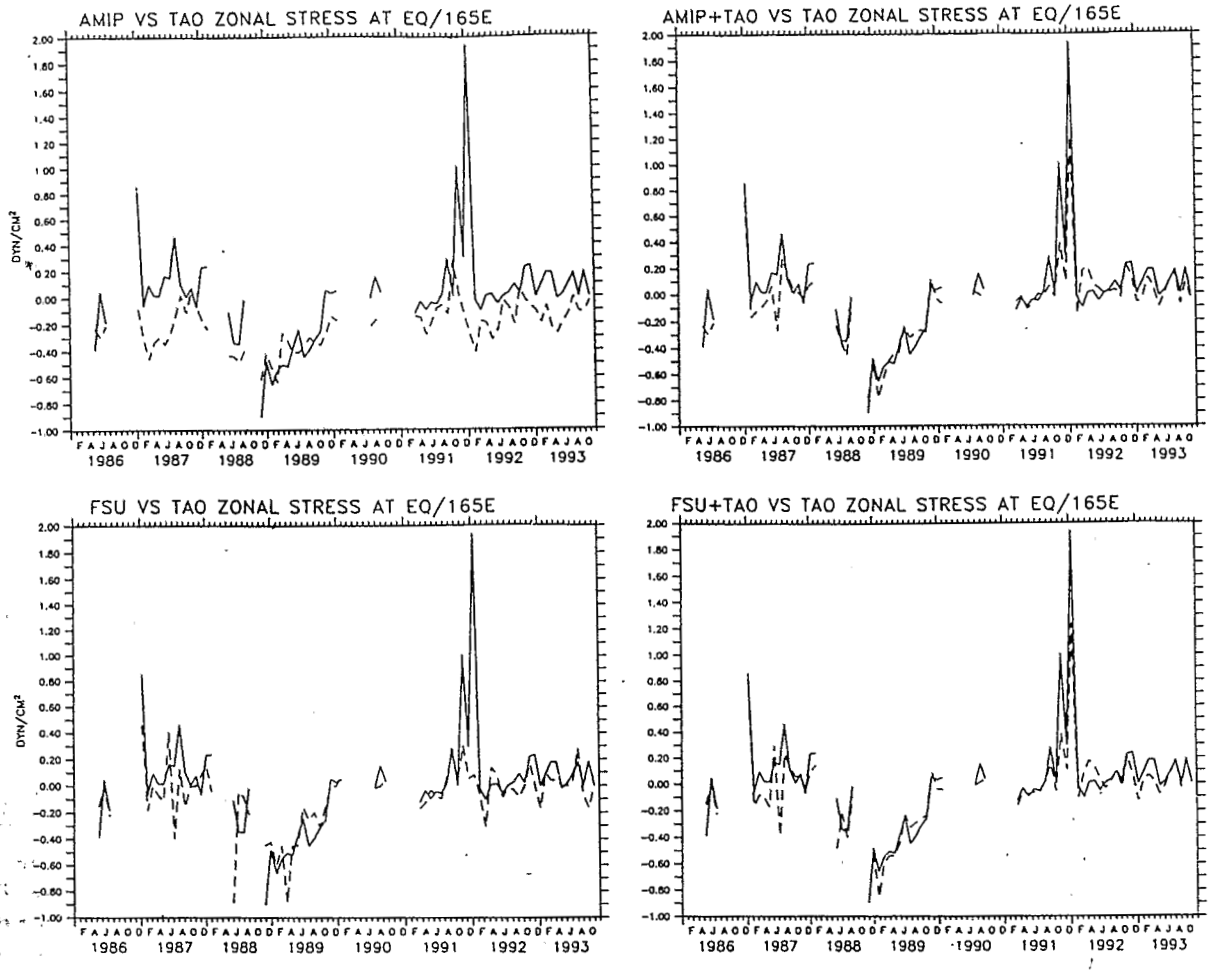

Figure 3 - (a-top left) : wind stress time series at EQ/165E for AMIP9 (dashed) and TAO (plain). (b-top right) : same but for AMIP9+TAO (dashed) versus TAO (plain). (c-bottom left) : same with FSU (dashed) versus TAO (plain). (d-bottom left) : same with FSU+TAO (dashed) versus TAO (plain).

Correlation maps between the baseline forcings and the improved winds (not shown here) show that, for AMIP9, the major impact of TAO is located north of the equator from 110°W to 160°E and for FSU, the principal influence is east of 140°W. The addition of TAO observations seems to have a greater impact on the AMIP9 winds. The region where AMIP9 and FSU winds are the most inconsistent is the eastern equatorial Pacific (Figure 4a) and the addition of TAO observations into the two baseline forcings brings the AMIP9 and FSU forcings in closer agreement in the equatorial band. (Figure 4b)

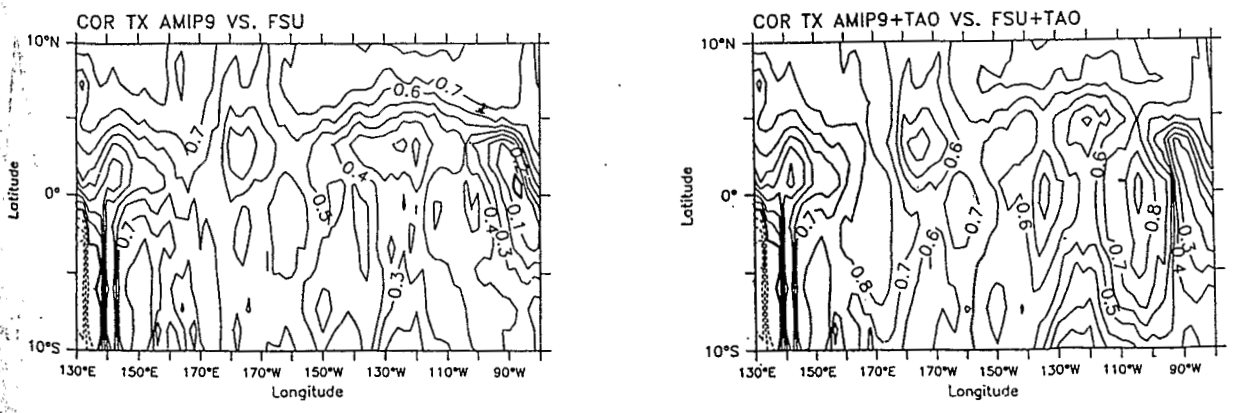

Figure 4 - (a) correlation maps between FSU and AMIP9 (left) and (b) between FSU+TAO and AMIP9+TAO.

EVALUATION OF SEA LEVEL SOLUTIONS

The previous wind data sets are used to force a 2 vertical mode linear model of the equatorial Pacific (Cane and Patton, 1984; Busalacchi and Cane, 1985). The phase evolution of the resulting sea-level solutions are compared in Figure 5. It can be seen that the major discrepancies between the sea-level solutions driven by the baseline forcings are in the eastern Pacific and away from the equator in the central and western Pacific (Figure 5a). The principal influence of the TAO forcing is to modify the solutions in the same areas mentioned previously (not shown here). While not definitive, this suggests that TAO may have a positive impact in these regions. The addition of TAO to the baseline forcings brings the resulting sea-level solutions into closer agreeement (Figure 5b) and on spatial scale larger than just the improved winds (Figure 4b).

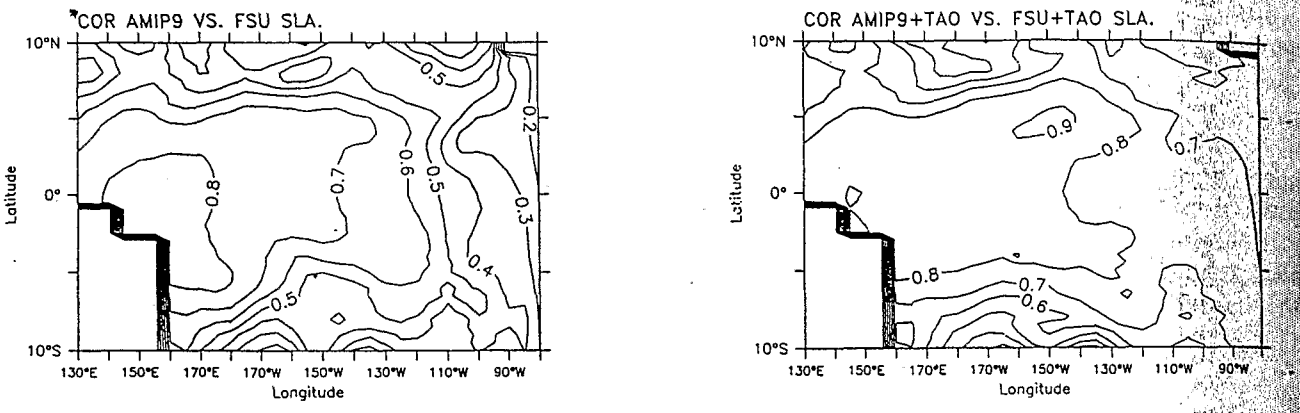

Figure 5 - (a) correlation maps between FSU and AMIP9-forced solutions (left) and (b) between FSU+TAO and AMIP9+TAO solutions.

Up to this point, we have only demonstrated those regions where the wind data and resulting sea-level anomalies are similar or different but comparisons with *in situ* observations are needed to assess quantitatively the impact of TAO. Inspection of individual modeled versus *in situ* time series at TAO locations EQ/165°E, EQ/140°W, EQ/110°W (not shown here) and at Santa Cruz (EQ/90°W) show that the addition of just a few TAO moorings has a significant impact on the simulation of the El Niño events during this time period (Figure 6). While the 86-87 El Niño is missed completely by the AMIP9 simulation at Santa Cruz (Figure 6a), the addition of some 10 TAO observations (Figure 1) brings the AMIP9+TAO solution in closer agreement with observations (Figure 6b) and with the FSU and FSU+TAO simulations (Figure 6c-d). From 89 onward, the addition of TAO winds to AMIP9 enables the simulations of the 91-92-93 El Niño (Figure 6b) otherwise missed (Figure 6a).

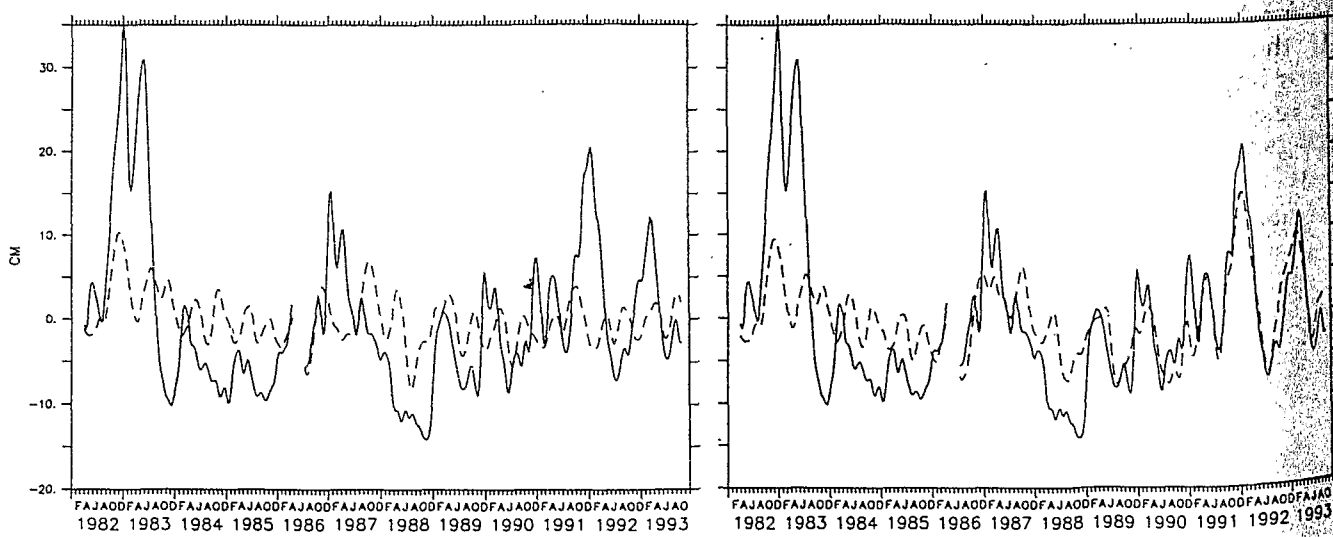

Figure 6 - observed sea-level anomalies (plain curve) versus modeled (dashed curve) at Santa Cruz (EQ/90°W) for the AMIP9 solution (a-left) and AMIP9+TAO (b-right)

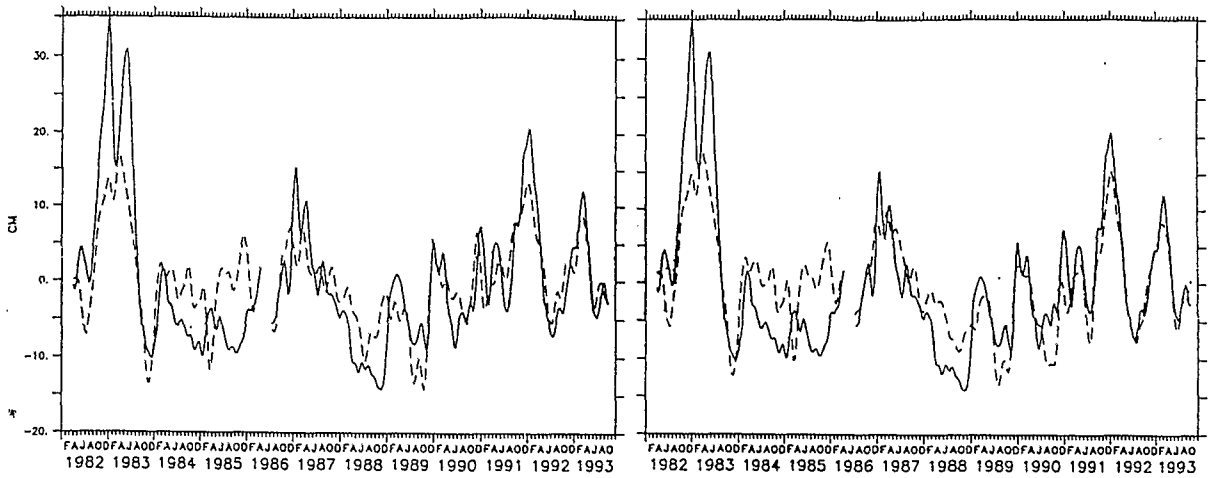

Figure 6 - observed sea- level anomalies (plain curve) versus modeled (dashed curve) at Santa Cruz (EQ/90°W) for FSU solution (c-left) and FSU+TAO (d-right).

At all three TAO dynamic height locations, the addition of TAO has a positive impact on both the FSU and AMIP solutions (Table 1) and moving eastward to Santa Cruz, there is a clear degradation of the AMIP solutions (Table 1). As a whole, the mean statistics over the 4 validation points (Table 1, last column) show that the addition of TAO has a positive impact on the AMIP9 and the FSU solutions and that the AMIP9+TAO and FSU+TAO solutions are almost undistinguishable.

Table 1: Correlation coefficients between modeled solutions (first column) and observations (first line) computed over 1984-1993.

	Santa Cruz	EQ/110°W	EQ/140°W	EQ/165°E	mean
AMIP9	0.13	0.36	0.63	0.65	0.44
AMIP9+TAO	0.77	0.84	0.79	0.72	0.78
FSU	0.72	0.76	0.72	0.64	0.71
FSU+TAO	0.73	0.82	0.78	0.73	0.77

Equatorial sections of TAO dynamic height anomalies (Courtesy of Mike McPhaden), AMIP9, AMIP9+TAO, FSU and FSU+TAO solutions (not shown here) further confirm that AMIP9 lacks most of the adequate high frequency wind variability that generates Kelvin waves. The addition of TAO remedies this situation and Kelvin waves are clearly seen in the AMIP9+TAO, FSU, and FSU+TAO solutions. As the TAO array comes to its near full development in late 1992 (Figure 2), these three latter solutions exhibit a variability similar to the observed and from which the AMIP solution strongly diverges.

We have a year overlap of these results with the first year of the TOPEX/POSEIDON mission with which to assess the spatial structure of sea-level simulations. As inferred previously, AMIP9 does poorly in the eastern Pacific (Figure 7a). The addition of TAO (Figure 7b) remedies the poor quality of the AMIP9 solution in the east and brings it to the level of the FSU and FSU+TAO solutions (Figure 7c-d). Yet, there is a V-shaped region of lower correlations, beginning in the central Pacific, near 150°W, spreading poleward and eastward. This appears to be a model deficiency as pointed out in the comparison between *in-situ* TOGA-TAO dynamic height and TOPEX/POSEIDON sea-level anomalies (Figure 7e).

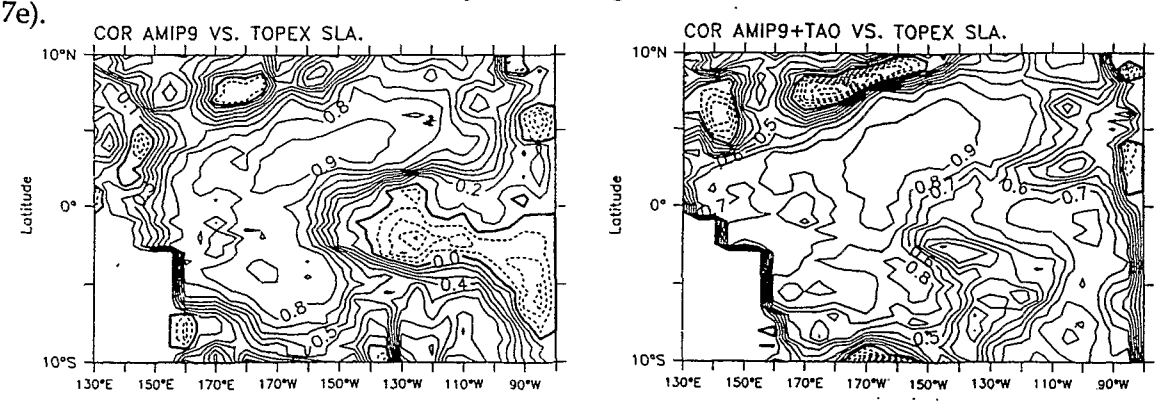

Figure 7 - Correlations between sea-level anomalies from TOPEX and the AMIP9 solution (a-left) and the AMIP9+TAO solution (b-right) over the 09/92-11/93 period. TOPEX is processed as in Menkes et al. (1995).

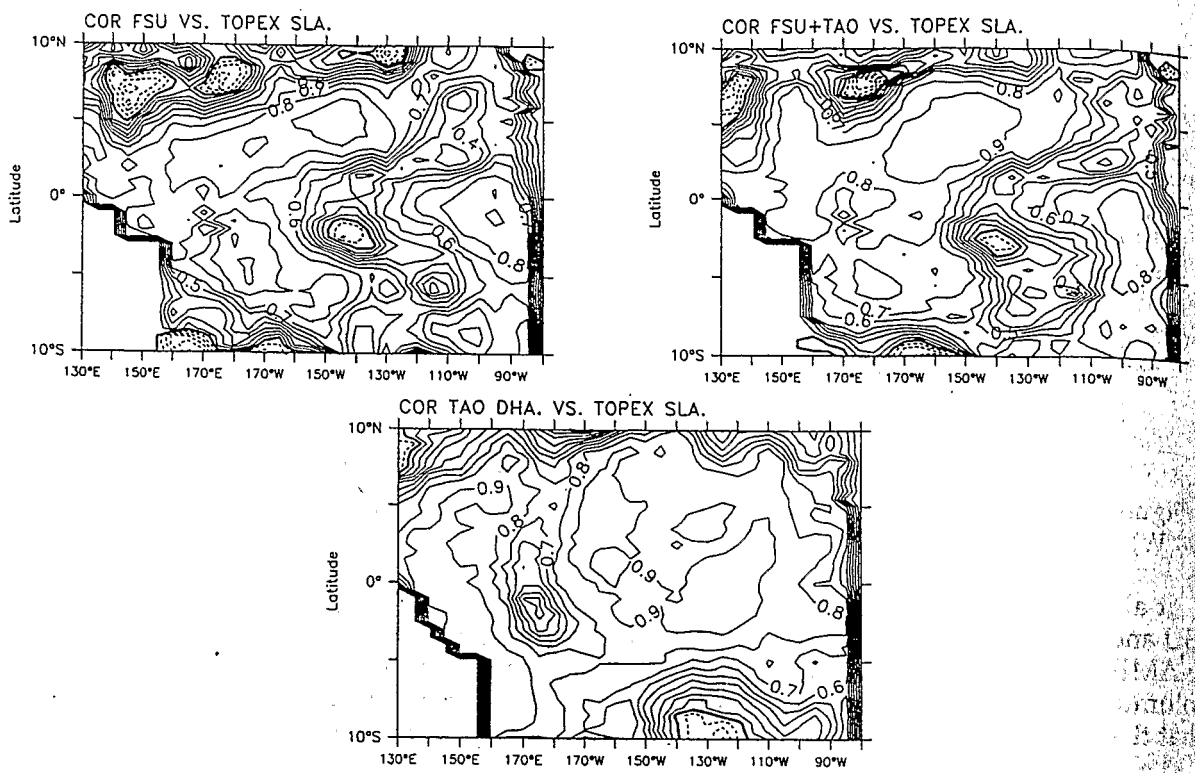

Figure 7 - Correlations between sea-level anomalies from TOPEX and the FSU solution (c-top left), the FSU+TAO solution (d- top right) and (e-bottom) TAO dynamic height anomalies (Menkes et al., 1995).

CONCLUSION

The addition of a few TAO winds into the AMIP9 wind remedies the poor quality of the AMIP9-forced sea-level simulations within a few degrees off the equator. TAO winds also have a positive impact on the FSU simulations. This applies within the equatorial wave guide, the region for which TAO was designed and does not take into account the extra latitudinal coverage of the wind field provided by the FSU winds.

As the TAO array increases and comes to its near-full deployment in the later years, the beneficial impact of TAO winds on sea-level simulations increases to the point where AMIP9+TAO and FSU+TAO basin-wide simulations are of comparable quality. This suggests that the inadequate patterns found in the AMIP9 wind (Ji and Smith, 1995) can be compensated by the addition of TAO winds for equatorial Pacific simulations. It is therefore suggested that atmospheric data assimilation schemes give a heavy weight to TAO winds.

To investigate the role of TAO winds further, it remains to be shown what impact TAO observations may have on simulations of the full ocean dynamics and thermodynamics and on ENSO prediction.

REFERENCES

Busalacchi A. and Cane, M. A., 1985: Hindcasts of sea level variations during the 1982-83 El Niño. J. Phys. Oceanogr., 15, 213-221.

Cane, M. A. and Patton R. J. , 1984: A numerical model for the low-frequency equatorial dynamics. J. Phys. Oceanogr., 14, 1853-1863.

Hellerman S. and Rosenstein, M., 1983: Normal monthly wind stress over the world with error estimates. J. Phys. Oceanogr., 13, 1093-1104.

Ji M. and Smith, T. M., 1995: Ocean model response to temperature data assimilation and varying surface wind stress: intercomparisons and implications for climate forecast, Monthly Weather Rev., in press

Liu W. T., Katsaros K. B. and Businger J. A., 1979. Bulk parametrisation of air-sea exchanges of heat and water vapor including the molecular constraints at the interface. J. Phys Oceanogr., 10, 1722-1735.

Menkes, C., Boulanger, J.-P. and Busalacchi, A. J., 1995: Evaluation of TOPEX/POSEIDON and TOGA-TAO sea level topographies and their derived geostrophic currents. J. Geophys. Res., submitted.

PROCEEDINGS OF THE

International Scientific Conference on

TROPICAL OCEAN GLOBAL ATMOSPHERE (TOGA) Programme

(2-7 April 1995, Melbourne, Australia)

WCRP-91 - WMO/TD No. 717

VOLUME I

December 1995